Design and Real Time Implementation of Fractional Order Proportional-Integral Controller (PI^{λ}) in A Liquid Level System

K.Vaithiyanathan
Department of Chemical Engineering, Annamalai University
Annamalainagar 608002, Tamilnadu, India
E-mail: vkvk58@yahoo.co.in

P.K.Bhaba(Corresponding author)
Department of Chemical Engineering, Annamalai University
Annamalainagar 608002, Tamilnadu, India
E-mail: pkbhaba@gmail.com

Received: October 8, 2011 Accepted: October 30, 2011 Published: December 1, 2011
doi:10.5539/mas.v5n6p188 URL: http://dx.doi.org/10.5539/mas.v5n6p188

Abstract

This research article deals with the design and real time implementation of a fractional order Proportional-Integral controller (PI^{λ}) for a Liquid Level System (LLS). The system is approximated as a First Order Plus Time Delay (FOPTD) model. The equivalent transfer function of this system in polynomial format is considered here for controller design. Expressions for controller parameters (K_P and K_I) in terms of frequency (ω) and fractional order (λ) are derived from the Fractional Order Characteristic Polynomial (FOCP) of the closed loop system. The global stability region based on K_P and K_I for each λ is constructed. Average values of K_P and K_I, for each λ, are taken. Among these values, the best fit of $K_{P\ average}$ and $K_{I\ average}$ and corresponding λ are identified by means of optimization techniques. The real time implementation of PI^{λ} controller with the identified controller settings in LLS is done. The PI^{λ} controller performances are analyzed in terms of ISE and IAE. A comparison of this control strategy with other conventional based controller techniques is made. PI^{λ} controller outperforms the conventional PI controllers. In addition the load disturbance studies are also carried out and it justifies the supremacy of PI^{λ} controller.

Keywords: Fractional order Proportional-Integral controller (PI^{λ}), LLS, Global stability region

1. Introduction

PID controllers belong to the dominating form of feedback industrial controllers and there is a continuous effort to improve their quality and robustness. Design and tuning of PID controllers have been a large research horizon ever since Ziegler and Nichols presented their methods in 1942. Specifications, stability, design, applications and performance of the PID controller have been widely treated since then. In recent years, there is an increasing number of studies related to the application of fractional controllers in many areas of science and engineering. Fractional Order PID (FO-PID) controllers could benefit the industry significantly with a wide spread impact when FO-PID parameter tuning techniques have been well developed. This fact is due to a better understanding of the Fractional Calculus (FC) revealed by studies on viscoelasticity, damping, chaos, diffusion, wave propagation, percolation and irreversibility.

The FC concepts are adapted to frequency-based methods. The introduction of fractional order calculus idea to conventional controller design extends the opportunity of added performance improvement. The frequency response and the transient response of the non-integer integral and its application to control systems was introduced by Manabe (Manabe, S, 1960). Oustaloup (Oustalouo,A, 1990) studied the fractional order algorithms for the control of dynamic systems and demonstrated the superior performance of the CRONE (Commande Robuste d'Ordre Non Entier) method over the PID controller.

Podlubny (Igor.Podlubny, 1999) proposed a generalization of the PID controller, namely the $PI^{\lambda}D^{\mu}$ controller, involving an integrator of the order λ and a differentiator of the order μ. He also demonstrated that the response of this type of controller is better as compared to the classical PID controller. Research activities are now focused to develop new tuning rules for fractional controllers for real systems. Some of these techniques are based on an extension of the classical PID control theory. An optimal fractional order PID controller based on specified gain margin and phase margin with a minimum ISE criterion has been designed by using a optimization techniques.

In general, the transfer function Gc(s) of a PI^{λ} controller is defined as

$$G_C(s) = \frac{U(s)}{E(s)} = K_P + K_I S^{-\lambda} + K_D S^{\mu} \qquad (\lambda, \mu > 0)$$

Where E(s) is the error signal and U(s) is controller's output. The parameters (K_P, K_I and K_D) are the proportional, integral and derivative gains of the controller, respectively. The $PI^{\lambda}D^{\mu}$ algorithm is represented by a fractional integro-differential equation of type:

$$U(t) = K_P e(t) + K_I D^{-\lambda} e(t) + K_D D^{\mu} e(t) \qquad (\lambda, \mu > 0)$$

Clearly, depending on the values of the orders λ and μ, we get an infinite number of choices for controller's type (defined through the (λ, μ)–plane). Conventional systems are derived from differential equations of integer order whereas fractional order systems are derived from fractional order differential equations. Since PID control is popular in many industry sections, $PI^{\lambda}D^{\mu}$ controller should provide additional potentials to achieve better performance. In this work, an attempt is made for the design and real time implementation of a PI^{λ} controller of the form $C(S) = K_P + \frac{K_I}{S^{\lambda}}$ for the integer order Liquid Level System (LLS). Here, three parameters can be tuned in this control structure (K_P, K_I and λ).

This paper is organized as follows: In Section 2, PI^{λ} controller design is explained. Experiments and analysis of real time implementation of PI^{λ} controller for Liquid Level System (LLS) is discussed in Section 3. Results and discussions and concluding remarks are given in Section 4 & 5.

2. Design of PI $^{\lambda}$ controller

The transfer function of the process, after approximating the delay using Pade first order approximation, is expressed in polynomial format as

$$G(S) = \frac{N(S)}{D(S)} = \frac{(n_1 s + n_0)}{(d_2 s^2 + d_1 s + d_0)} \qquad (1)$$

The transfer function of the $PI^{\lambda}D^{\mu}$ controller is

$$C(s) = \frac{U(s)}{E(s)} = K_P + \frac{K_I}{S^{\lambda}} + K_D S^{\mu} \quad \text{where } (\lambda, \mu > 0\ ) \qquad (2)$$

Here the differential element is not considered (i.e) K_D=0, then the $PI^{\lambda}D^{\mu}$ controller becomes PI^{λ} controller

$$(i.e)\ \ C(s) = \frac{U(s)}{E(s)} = K_P + \frac{K_I}{S^{\lambda}} \quad \text{where } (\lambda > 0) \qquad (3)$$

The output of the feedback PI^{λ} controller with a process (Ref: Figure 1) is given as

$$y = \frac{C(s)G(s)}{1 + C(s)G(s)} r \qquad (4)$$

The denominator of equation (4) represents the Fractional Order Characteristic Polynomial (FOCP) of the closed loop system.

$$\text{(i.e) FOCP=P(s)=1+C(s)G(s)=0} \qquad (5)$$

Substituting equations (1) and (3) in (5), FOCP is written as (Bhaba et al., 2007; Hamamci et al., 2008)

$$P(s) = (s^{\lambda})(d_2 s^2 + d_1 s + d_0) + (K_P s^{\lambda} + K_I)(n_1 s + n_0) = 0 \qquad (6)$$

Replacing s=jω, equation (6) becomes

$$P(\mathrm{j\omega}) = \left[(j\omega)^{\lambda}\right] * \left\{d_2 (j\omega)^2 + d_1 (j\omega) + d_0\right\} + \left\{K_P (j\omega)^{\lambda} + K_I\right\} * \left[n_1 (j\omega) + n_0\right] = 0 \qquad (7)$$

Using mathematical identity, equation (7) is written as

$$P(jw) = \left\{ \begin{array}{l} d_2(\omega)^{\lambda+2}\left[Cos(\lambda+2)(\pi/2) + jSin(\lambda+2)(\pi/2)\right] + \\ \left[d_1 + K_P n_1\right](\omega)^{\lambda+1}\left[Cos(\lambda+1)(\pi/2) + jSin(\lambda+1)(\pi/2)\right] + \\ \left[d_0 + K_P n_0\right](\omega)^{\lambda}\left[Cos(\lambda)(\pi/2) + jSin(\lambda)(\pi/2)\right] + \\ K_I n_1 \omega j + K_I n_0 \end{array} \right\} = 0 \tag{8}$$

Equating Real and Imaginary parts of P(jω) to zero,

Real part is given as follows:

$$\begin{array}{l}\left[d_2(\omega)^{\lambda+2}\right]Cos\left[(\lambda+2)(\pi/2)\right] + \left[d_1 + K_P n_1\right](\omega)^{\lambda+1} Cos\left[(\lambda+1)(\pi/2)\right] + \\ \left[d_0 + K_P n_0\right](\omega)^{\lambda} Cos\left[(\lambda)(\pi/2)\right] + K_I n_0 = 0\end{array} \tag{9}$$

And Imaginary part is given as:

$$\begin{array}{l}\left[d_2(\omega)^{\lambda+2}\right]Sin\left[(\lambda+2)(\pi/2)\right] + \left[d_1 + K_P n_1\right](\omega)^{\lambda+1} Sin\left[(\lambda+1)(\pi/2)\right] + \\ \left[d_0 + K_P n_0\right](\omega)^{\lambda} Sin\left[(\lambda)(\pi/2)\right] + K_I n_1 \omega = 0\end{array} \tag{10}$$

Solving equations (9) and (10), the expressions for KP and KI (PI λ controller parameters) are derived as

$$K_P = \frac{\left[Sin(\lambda)(\pi/2)\left\{\omega^2(d_2 n_0 - d_1 n_1) - d_0 n_0\right\} + Cos(\lambda)(\pi/2)\left\{\omega(d_0 n_1 - d_1 n_0) - \omega^3(d_2 n_1)\right\}\right]}{Sin(\lambda)(\pi/2)\left[n_1^{\,2}\omega^2 + n_0^{\,2}\right]} \tag{11}$$

$$K_I = \frac{\omega^{\lambda}\left[\omega^3(n_1 d_2) + \omega(n_0 d_1 - n_1 d_0)\right]}{Sin(\lambda)(\pi/2)\left[n_1^{\,2}\omega^2 + n_0^{\,2}\right]} \tag{12}$$

ω changes from 0 to ω_{maximum}, whose value is determined by substituting $K_I = 0$ in equation (12). Using equations (11) and (12), K_P and K_I values are calculated for each value of λ (varying from 0.1 to 1.9, in steps of 0.1), by substituting ω from 0 to ω_{maximum}. A stability curve in the K_P-K_I plane is constructed for each λ (Ref: Figure 2). All regions bounded in between stability curve and the stability line is represented as Global Stability Region. From the Global Stability Region, the average values of K_P and K_I corresponding to the each value of λ is obtained Among these values , the best fit of $K_{P\ \text{average}}$ and $K_{I\ \text{average}}$ and corresponding λ are identified by means of optimization techniques.

3. Experiments and Analysis

3.1 Experimental setup

The functional diagram of Liquid Level System is shown in Figure 3. The setup consists of process tank, collection tank, variable speed pump, RF capacitance level sensor and Interface card VMAT01. The variable speed pump is attached to the collection tank and speed of the pump is controlled by Thyristor Power Control (TPC) unit. The specifications of all the above said major hardware parts of the system are given in Table 1. Water in the collection tank is pumped to the process tank by means of a variable speed pump. The level in the process tank is measured by RF capacitance level sensor and it converts the physical quantity of level to current signal which in turn is converted into a voltage signal of 0 to 5 V by I / V converter. A newly designed VMAT01 interface board consisting of a multifunction, high speed, Analog to Digital Converter (ADC) and Digital to Analog Converter (DAC) is interfaced with the PC-AT Pentium 4. The special feature of VMAT01 is that it can run the real time control algorithms in simulink tool of MATLAB platform directly.

3.2 Model parameters identification

In open loop scheme, after the level in the tank reaches the steady state, a step magnitude of 5% DAC output to the variable speed pump is given .The level in the tank varies and this variation in level is recorded against time until a new steady state is reached. This recorded data is converted into fractional response and plotted against time to get the process reaction curve. The parameters for the model of LLS are estimated from this reaction curve using S-K (Sunderasan,K.R and Krishnaswamy,P.R, 1978) identification method.

3.3 Real time implementation of PI $^{\lambda}$ controller in LLS

For real time implementation of both the conventional and PI$^{\lambda}$ controller in LLS, their corresponding simulink blocks are used. The latter PI$^{\lambda}$ block is incorporated by using VALERIO's NINTEGER (nipid) (Valerio,D , 2005; Ivo Petras , 2009) MATLAB toolbox.

Real time runs are carried out in LLS with conventional control schemes and PI$^{\lambda}$ control scheme separately. Three different conventional tuning rules (Ziegler-Nichols, 1942), (Padmasree-Srinivas-Chidambaram, 2004) and (Hsiao Ping HUANG-Jyh Cheng Jeng-KUO Yuan Luo,2005) are used in this work for estimating conventional PI controller settings . Set point tracking of magnitudes (±5% & ±10%) at three nominal operating points 40%, 55%, and 70% of level for all the control scheme in this system are performed. In addition, Load Rejection test at two nominal operating points 40% and 55% of level are also carried out. Tracking responses in both cases are recorded.

4. Results and discussions

4.1 Construction of Global stability region

The model parameters of LLS, as detailed in section 3.2, are identified as Process Gain Kp=4.31, Process Time constant τ_p=22.8s and time delay L =6s. These model parameters are used to estimate the conventional PI controller parameters for three conventional tuning rules and they are listed in Table 2. From expressions (11) and (12) of section 2, K_P and K_I values for different λ (varying from 0.1 to 1.9 in steps of 0.1) and corresponding frequency ω (varying from 0 to ω maximum) are computed . The global stability region based on K_P and K_I for different λ are constructed. A sample construction of Global stability region for λ=0.5 is given in Figure 2. Average values of K_P and K_I, for each λ, are taken. Among these values, the best fit of K P average and K I average and corresponding λ are identified by means of optimization techniques. The identified $K_{Paverage}$, $K_{Iaverage}$ and λ are listed as $K_{Paverage}$ =0.4639, $K_{I\ average}$ =0.2255, λ=0.5.

4.2 Performance of PI $^{\lambda}$ controller

With these values of conventional and PI$^{\lambda}$ controller parameters, real time runs are performed in LLS for set point tracking of ±5% & ±10% at the operating point 40% of level and load rejection test at the same operating point. The tracking responses are recorded in Figure 4 to Figure 5. From these Figures, controller performance indices such as ISE & IAE for each control schemes are estimated and values are tabulated in Table 3 & Table 4. From these tabulated values, it is observed that PI$^{\lambda}$ controller outperforms the conventional PI control techniques in both tracking cases.

To analyze the robustness of the proposed PI$^{\lambda}$ controller an experimental run at other operating points 55% & 70% of level in LLS are carried out .The results of set point tracking of ±5% & ±10% at these operating levels are recorded in Figure 6 to Figure 7. Load rejection test at 50% operating point with all controllers are carried out. The performance measures are given in Table 5 to 7 clearly indicates the supremacy of PI$^{\lambda}$ controller.

5. Conclusion

In this paper a fractional order PI (PI$^{\lambda}$) controller for an integer order liquid level system is proposed.

Expressions for two main parameters of PI$^{\lambda}$ controller (K_P and K_I) are developed in terms of frequency ω and fractional order λ. Global stability regions are constructed and best fit values of K_P and K_I are identified by adapting optimization technique.

Real time runs with these controller parameters are carried out for various set point tracking and load rejection. Performance analysis of the proposed controller is done. In addition a comparison with other conventional tuning rules based PI controller is made. Result shows the supremacy of the proposed fractional controller PI$^{\lambda}$.

Acknowledgement

We are cheerfully showering our heartfelt thanks to Prof.S.E.Hamamci, Associate Professor, Department of Electrical-Electronics Engineering, Inonu University, Turkey for his help and valuable suggestion.

References

Aidan, O. *Handbook of PI and PID controller tuning rules*. (3rd ed). London: Imperial college Press, (Chapter 3).

Bhaba. P. K., Vaithiyanathan, K., & Hamamci, S. E. (2007). Design and implementation of PI$^{\lambda}$ controller in a liquid level system. *International Conference on Modeling and Simulation*. CIT, (CITICOMS 2007), Coimbatore, India. 27-29 August 2007, 1, 183-188.

Hamamci, S. E., Kanthabhabha, P., & Vaithiyanathan, K. (2008). *Computation of all stabilizing First order controllers for fractional order systems*. Procedings of 27th Chinese control conference, July 16-18, 2008. Kunming, Yunan, China. http://dx.doi.org/10.1109/CHICC.2008.4605635

Hamamci. S. E. (2008). Stabilization using fractional–order PI and PID controllers. *Nonlinear Dyn*, 51,329-343. http://dx.doi.org/10.1007/S11071-007-9214-5

Huang, H. P., Jeng, J. C., & Luo, K. Y. (2005). Auto-tune system using single run relay feedback test and model-based controller design. *Journal of Process Control*, 15, 713-727. http://dx.doi.org/10.1016/j.jprocont.2004.11.004

Igor, P. (1999). Fractional–order systems and $PI^{\lambda}D^{\mu}$-controllers. *IEEE Trans. Automatic control*. 44(1), 208-214. http://dx.doi.org/10.1109/9.739144

Ivo, P. (2009). Fractional-order feedback control of a DC motor. *Journal of Electrical Engineering*, 60(3), 117-128.

Manabe, S. (1960). The non-integer integral and its application to control systems. *J. of IEE of Japan*, 80(860), 589-597.

Oustaloup, A. (1990). CRONE control principle, synthesis, performances with nonlinearities and robustness. *Control and information sciences*, 144, 767-777. http://dx.doi.org/10.1007/BFb0120098

Padma Sree, R., Srinivas, M. N., Chidambaram, M. (2004). A Simple method of tuning PID controllers for sTable and unsTable FOPTD systems. *Computers and chemical Engineering*, 28, 2201-2218. http://dx.doi.org/10.1016/j.compchemeng.2004.04.004

Sunderasan, K .R., & Krishnaswamy, P. R. (1978). Estimation of time delay , time constant parameters in time, frequency and laplace domains. *Can J. Chem*. Eng, 56, 257-262. http://dx.doi.org/10.1002/cjce.5450560215

Valerio, D. (2005). Toolbox ninteger for Matlab, v.2.3. [Online] Available: http://web.ist.utl.pt/duarte.valerio/ninteger/ninteger.htm

Table 1. Specification of Hardware parts in LLS

Variable speed motor pump		Process tank		Collection tank	
Type	Tullu-80	Material	Acrylic	Material	Mild steel
Speed	6500 RPM	Capacity	3.5 litres	Capacity	10 litres
Discharge	800 lit/hr	Height / Diameter	30 cm 15 cm		

Table 2. Conventional PI Controller Parameters

Controller Parameters	ZN-PI Controller	CDM-PI Controller	HUANG-PI Controller
K_P	0.7935	0.74124	0.487
K_I	0.0397	0.03215	0.021

Table 3. Performance measures of PI^{λ} controller in terms of ISE and IAE at operating point 40% of level

Set Point Tracking cases	I S E	I A E
+05%	146.1649	70.09804
-05%	271.6551	105.1961
+10%	648.6351	145.2941
-10%	1116.148	210.7843

Table 4. Load Rejection: Performance measures of Controllers at operating point 40% of level

TUNING RULES	I S E	I A E
PI^{λ} controller	49.05975	55.2969
ZN – PI controller	1804.693	458.4319
CDM – PI controller	74.43493	80.7867
HUANG – PI controller	226.6837	141.9628

Table 5. Comparison of performance measures (ISE) of PI^{λ} controller with other conventional controllers

Operating point %	Set point tracking cases	PI^{λ} controller	ZN-PI controller	CDM-PI controller	HUANG-PI controller
40	+ 05%	146.1649	191.3014	194.5309	262.7332
40	-05%	271.6551	1075.807	447.9719	319.3283
40	+10%	648.6351	1345.29	1206.574	1097.382
40	-10%	1116.148	2095.463	1529.22	2279.388
55	+ 05%	193.4641	237.2933	211.1496	3632.82
55	-05%	192.1953	536.3706	494.233	321.3754
55	+10%	767.3875	1432.209	1225.135	4458.594
55	-10%	1101.72	1799.298	1592.762	1990.377
70	+ 05%	188.9177	235.2845	221.0592	269.272
70	-05%	194.3772	594.9154	291.955	345.7036
70	+10%	664.2061	1068.666	983.1603	1060.826
70	-10%	1034.371	1919.877	1342.561	1943.562

Table 6. Comparison of performance measures (IAE) of PI^{λ} controller with other conventional controllers

Operating point %	Set point tracking cases	PI^{λ} controller	ZN-PI controller	CDM-PI controller	HUANG-PI controller
40	+ 05%	70.09804	96.37255	86.76471	119.5073
40	-05%	105.1961	299.3137	151.2745	152.2544
40	+10%	145.2941	283.7255	253.5294	258.2341
40	-10%	210.7843	431.5686	286.8627	413.9206
55	+ 05%	85.4902	105.4902	88.23529	672.6466
55	-05%	86.86275	162.9412	155.098	132.3532
55	+10%	158.1373	303.0392	259.1176	705.8827
55	-10%	192.8431	333.2353	287.7451	350.0974
70	+ 05%	80.29412	102.8431	91.86275	115.7818
70	-05%	76.76471	174.6078	107.549	135.1948
70	+10%	129.8039	231.7647	201.9608	242.3536
70	-10%	177.2549	322.3529	242.3529	329.4137

Table 7. Load Rejection: Performance measures of Controllers at operating point 55% of level

TUNING RULES	I S E	I A E
PI^{λ} controller	59.08335	82.25
ZN – PI controller	116.0662	144.4128
CDM – PI controller	69.38932	98.9189
HUANG – PI controller	119.5995	118.5256

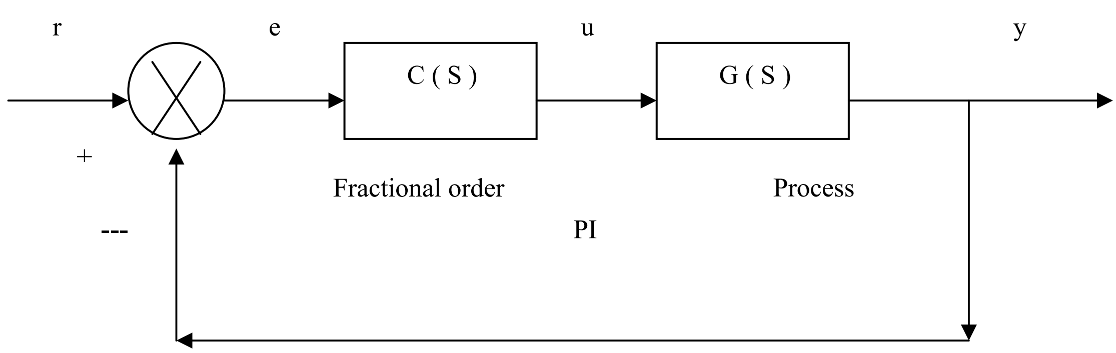

Figure 1. Block diagram representation of fractional order controller with process

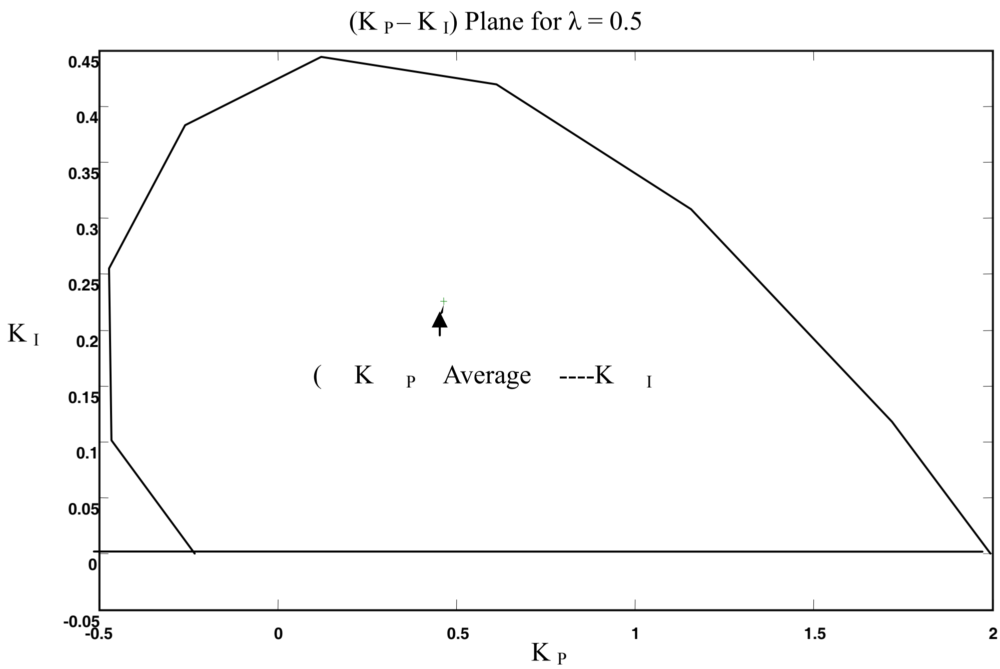

Figure 2. K_P-K_I plane for λ=0.5

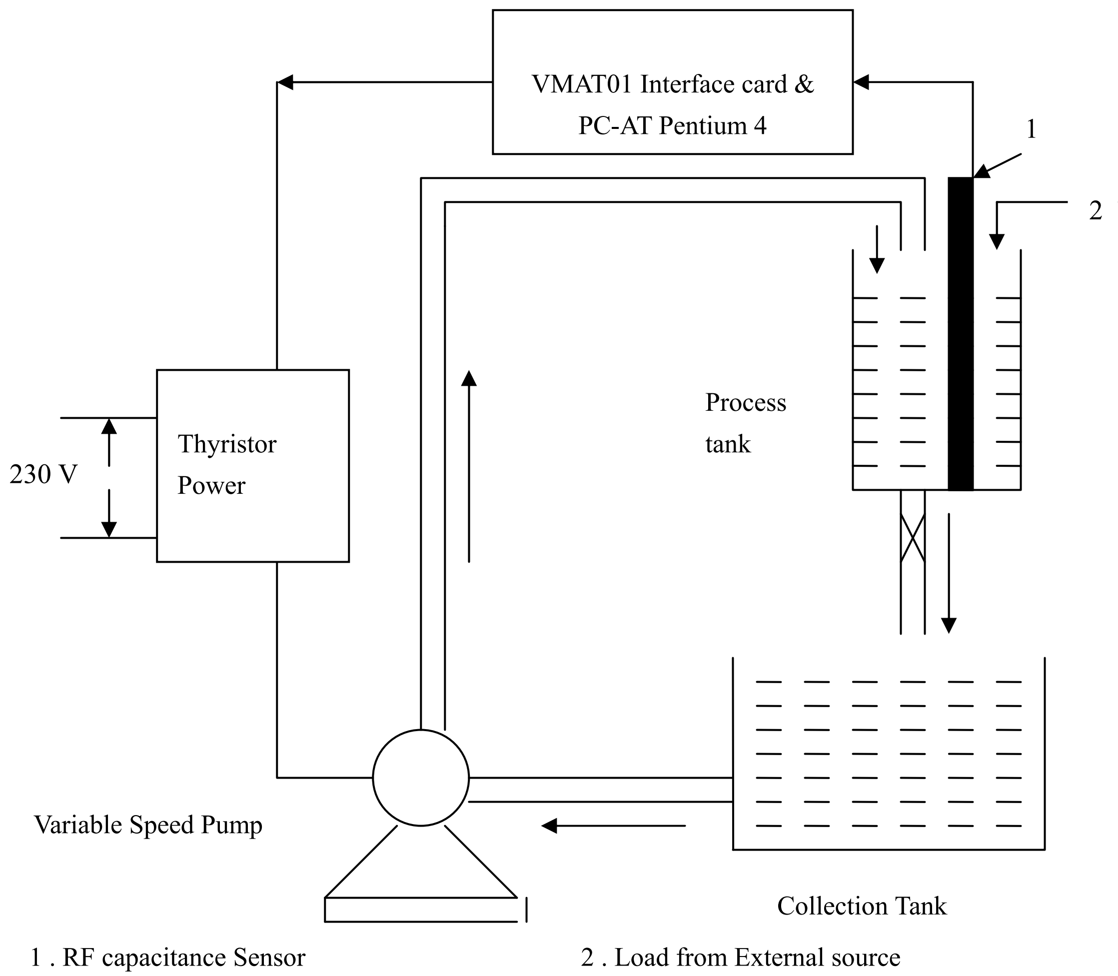

Figure 3. Functional Diagram of Liquid Level System

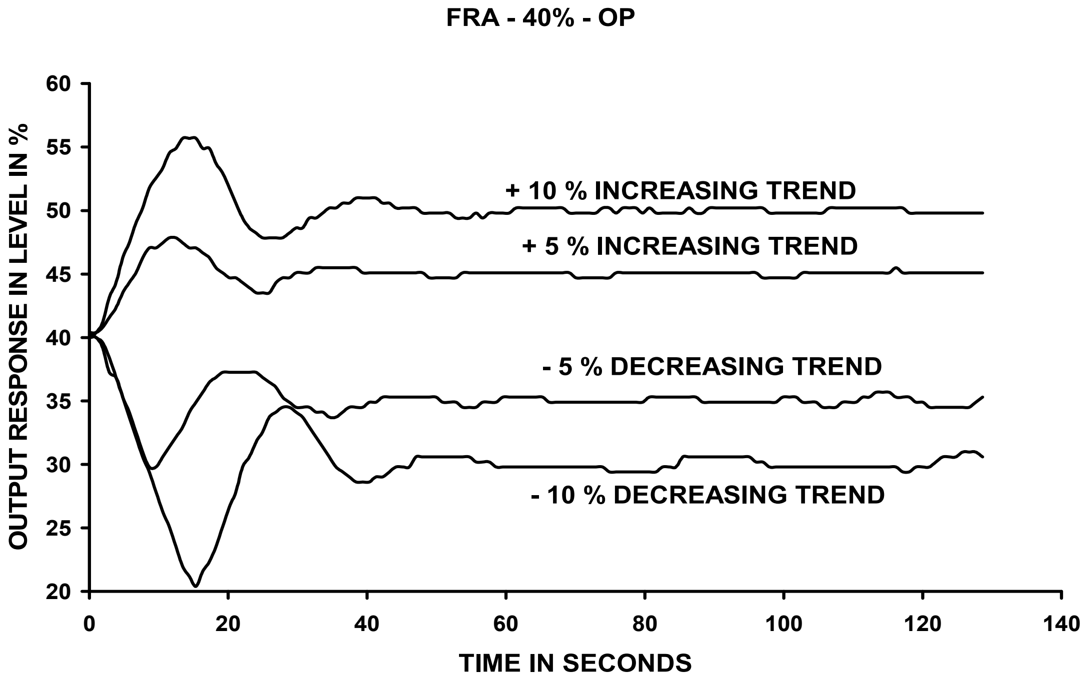

Figure 4. PI^{λ} Controller Servo responses for step sizes of ±5% and ±10% at the operating point 40% of level

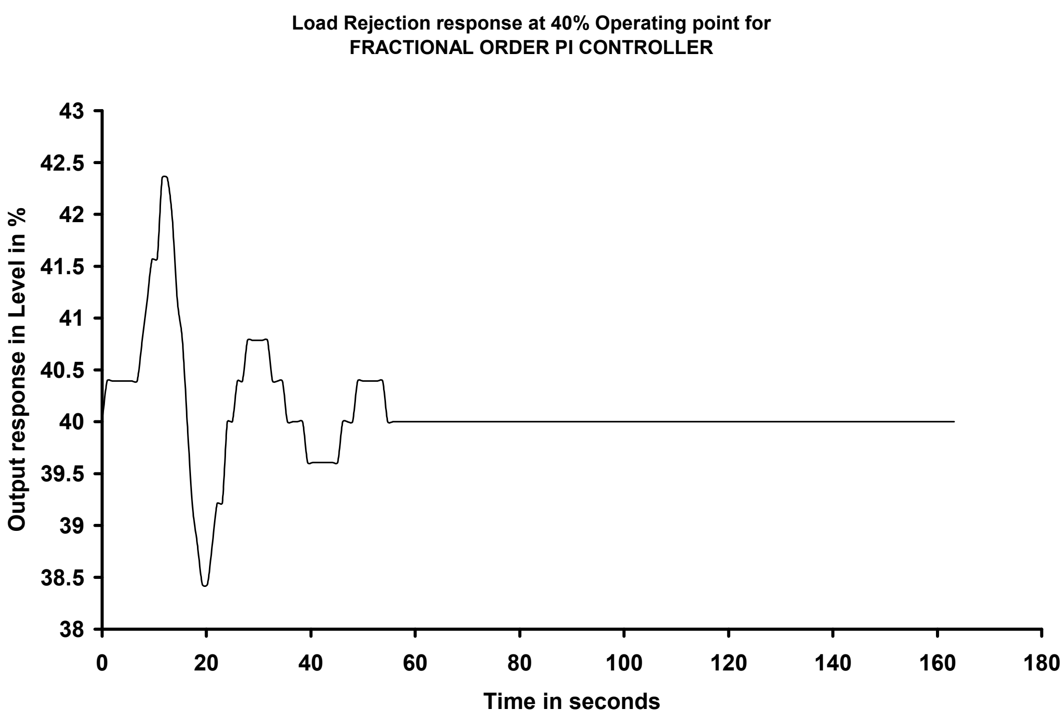

Figure 5. Load rejection response at the operating point 40% of level for Fractional Order PI controller

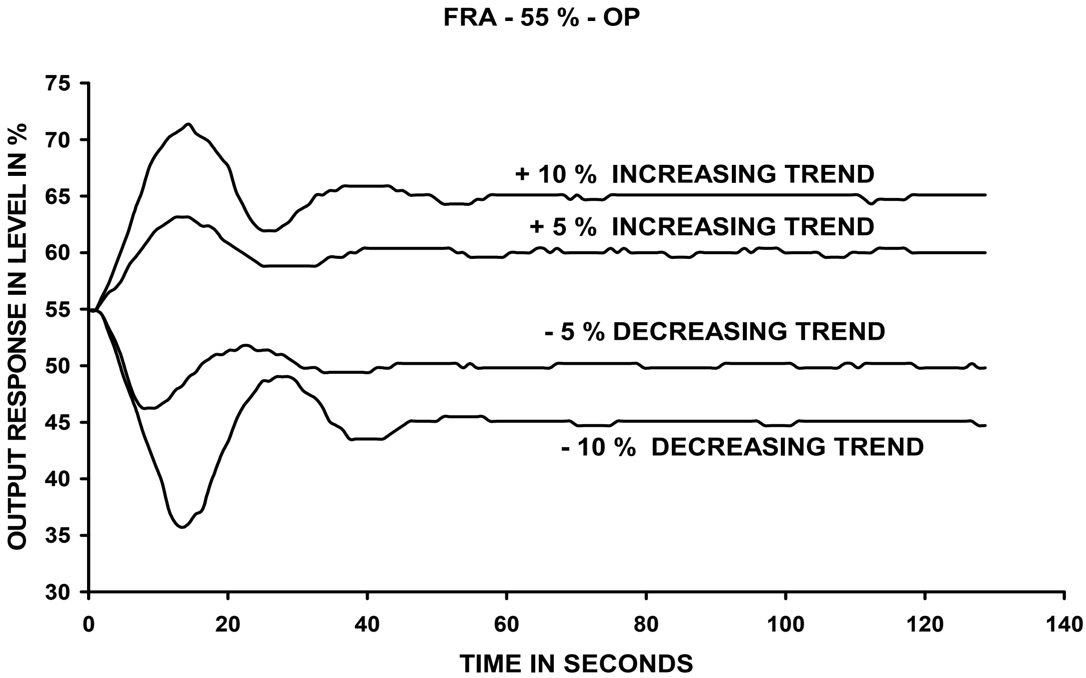

Figure 6. PI $^{\lambda}$ Controller Servo responses for step sizes of ±5% and ±10% at the operating point 55% of level

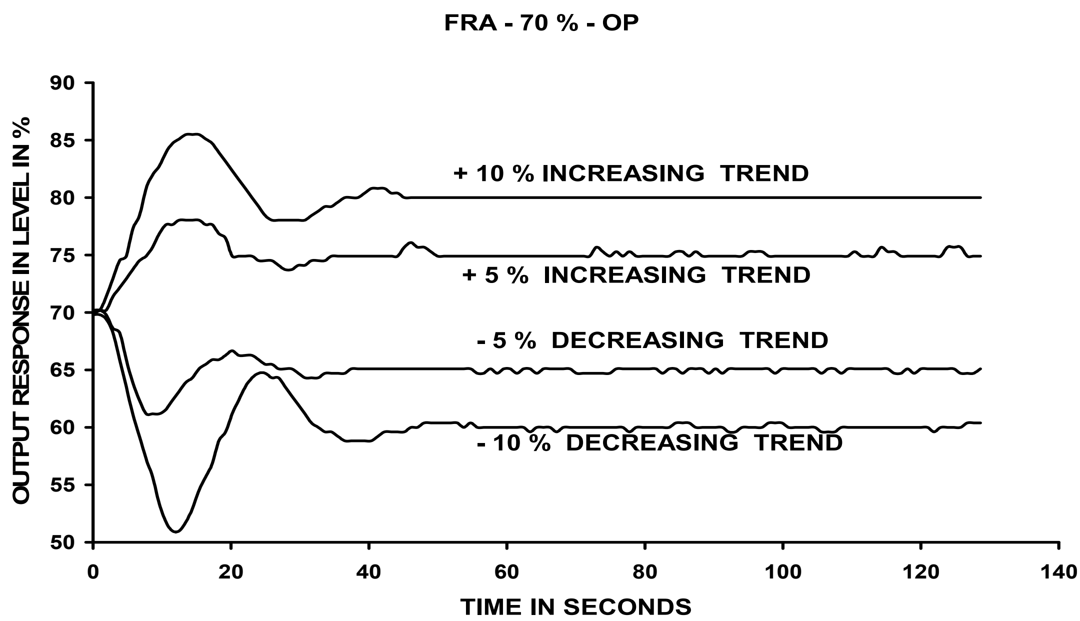

Figure 7. PI $^{\lambda}$ Controller Servo responses for step sizes of ±5% and ±10% at the operating point 70% of level